ME555 Design Optimization

Project Progress Report

Subject	ME555
Advisor	Emrah Bayrak
Submit Date	04/22/2016
Name	Jaehong Lee
	Hyunwoo Park

1. INTRODUCTION

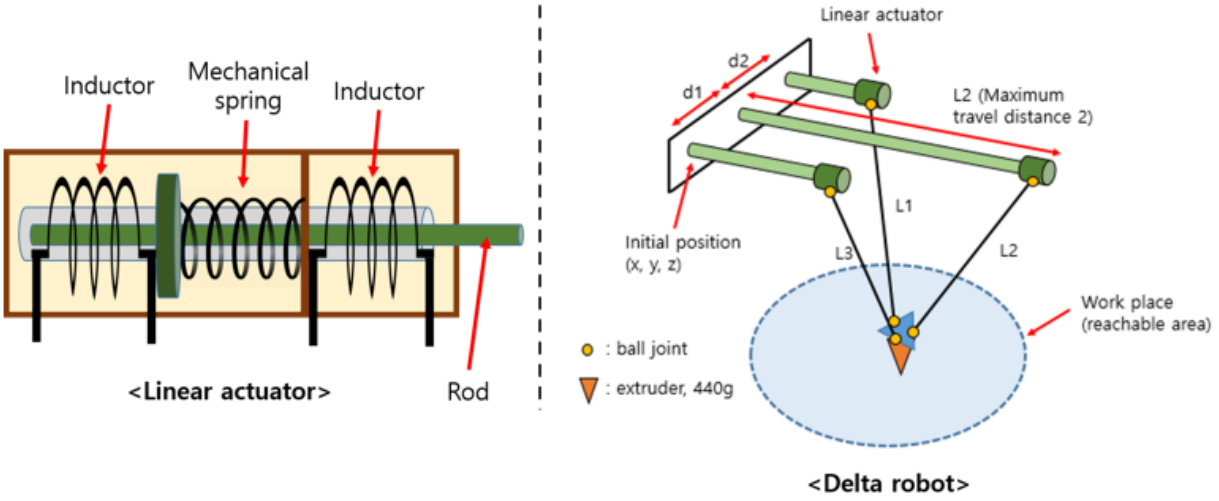

Conventional linear actuators mostly consists of motor with pinion and helical rack or ball nut with screw. These linear actuators are usually expensive and have limited force. In this project, the linear actuator is designed to produce large force. Solenoids are widely used as switching actuator. They have simple structure and relatively cheap to produce. Usually total travel of the plunger is very short; in most cases, it is limited to few centimeters only. However it can be extended by modifying design. Also if enough electromagnetic forces can be generated by applying enough current, the solenoid based linear actuator can generate the higher force compared to gear and motor based linear actuator.

A linear delta robot which has three parallel closed kinematic mechanism which links the base to the end effector. While the conventional delta robots have the revolute actuators and upper arms, the linear delta robot replaces these features with three parallel linear actuators. Also, the linear delta robot can be applied to 3D printing by replacing the end effector with an extruder. Compared to conventional 3D printer that uses cartesian system, delta robot based 3D printer has advantages. A 3D printer needs to be able to change it's direction instantly and as fast as possible. The heavier the moving part, the harder it is to make it stop or change direction in an instant. The benefit of a Delta is that the moving parts are lightweight so that it's easier to travel. That results in faster printing with greater accuracy.
The ultimate goal of this project is to design delta robot based 3D printer, which utilizes linear actuators.

2. PROJECT OVERVIEW

The objective of the project is to optimize the design of the 3D printer, so that its performance is improved to minimize time to make a 15 x 15 x 15 cm cubic block. The 3D printing system was divided into two sub-systems: linear actuator and linear delta robot. Each sub-system had specific objective as well. The linear actuators design was optimized to maximize force. On the other hand, the linear delta robot was designed to maximize the area of the workspace that is large enough for making a 15 x 15 x 15 cm (total volume = 3375 cm^3) cubic block.

3. SUBSYSTEM DESIGN

3.1 Design of a linear actuator

3.1.1 Problem statement

Objective of subsystem 1 is to design a solenoid based linear actuator which can generate maximized force with limited energy capacity. Electromagnetic force can generate powerful force if enough current can be applied. In this project, control input is neglected since it makes system more complex by adding many variables and parameters.

3.1.2 Modeling of a solenoid based linear actuator

Nomenclature

#	Symbol	Description	Unit
1	a	Length between solenoid and actuator end	(mm)
2	d_c	Copper wire diameter	(mm)
3	g	Air gap	(mm)
4	l_s	Length of the solenoid	(mm)
5	i	Current to the inductor	(A)
6	N	Number of coil turn	
7	d	Internal gap between shell	(mm)
8	λ	Flux linkage	(Wb-t)

9	μ_0	Magnetic constant	(N/A^2)
10	K	Spring constant	
11	M	Mass of the plunger	(g)
12	l_p	Plunger length	(mm)
13	d_p	Plunger diameter	(mm)
14	F_I	Induced force	(N)
15	x	Travel distance	(mm)
16	l	Length of the linear actuator	(mm)
17	t_s	Outer shell thickness	(mm)
18	R_t	Maximum range of travel	(mm)
19	μ_{ss}	Friction coefficient between steels	
20	g	Gravitational coefficient	(Nm)
21	x_0	Initial compressed length of the spring	(mm)

Model of the linear actuator

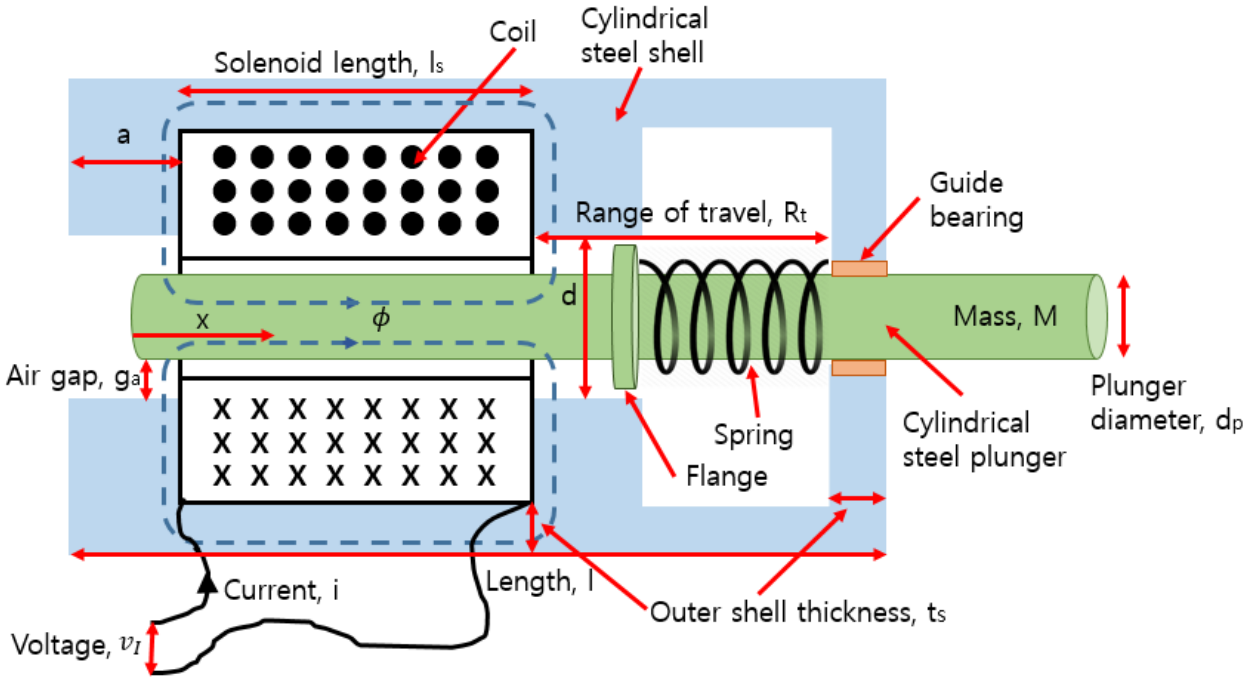

Figure 3.1: Structure of a solenoid based linear actuator

This linear actuator is solenoid based actuator and the difference between solenoid and this actuator is presence of the spring which has much higher spring constant.

Electrical subsystem is described by Kirchhoff's voltage law:

$v_I = R \cdot i + \frac{d\lambda}{dt}$, $\lambda = L(x) \cdot i$, where λ is the flux linkage and R is a resistance of the coil

$$v_I = R \cdot i + L(x)\frac{di}{dt} + i\frac{dL(x)}{dx} \cdot \frac{dx}{dt}$$

By assuming the relative permeability of the steel shell and other core elements to approach infinity, the total reluctance ($\Re$) can be distilled to the air gap contributions as a function of stroke (x) so that

$$\Re = \frac{g_a}{\mu_0 \pi d}\left(\frac{1}{a} + \frac{1}{x}\right) = \frac{g_a}{\mu_0 \pi d}\left(\frac{a+x}{x}\right)$$

The inductance (L) for the system is also given as a function of plunger stroke in the form

$$L(x) = \frac{N^2}{\Re} = \frac{\mu_0 \pi d a N^2}{g_a}\left(\frac{x}{a+x}\right)$$

Using the coenergy function and assuming a linear relationship between current (i) and total flux linkage (λ), induced force F_I can be expressed as

$$F_I = \frac{dWf}{dx} = \frac{i^2}{2}\cdot\frac{dL(x)}{dx} = \frac{i^2}{2}\cdot\frac{a^2\mu_0\pi d N^2}{g_a(a+x)^2}$$

Mechanical subsystem is defined by second Newton's law:

$$\sum F = M\cdot a = M\cdot\frac{dv}{dt} = M\cdot\frac{d^2x}{dt^2}$$

$$F_I - K(x-x_0) - \mu_{ss}Mg = M\cdot\frac{d^2x}{dt^2}$$

Net force, which need to be maximized is: $F = F_I - K(x-x_0) - \mu_{ss}Mg$

Also energy loss occurs when the direction of spring compression/extension is opposite direction with intended plunge movement.

$$E_{loss} = \frac{1}{2}(M + M_{extruder})\cdot v_{diff}{}^2 = \frac{1}{2}\cdot\left(0.00805\cdot\pi\cdot\left(\frac{d_p}{2}\right)^2 + M_{extruder}\right)\cdot l_p\cdot(v - v_{op})^2$$

$$= \frac{1}{2}\cdot\left(0.00805\cdot\pi\cdot\left(\frac{d_p}{2}\right)^2 + M_{extruder}\right)\cdot(R_t + l_s)\cdot(v - v_{op})^2$$

$M_{extruder}$ is a momentum from the extruder in the delta robot. E_{loss} term is not used in this subsystem analysis, but will be used in system level optimization.

3.1.3 Constraints

To simplify the problem, some parameters were determined before the start. For the coil, copper wire with 0.5mm diameter will be used.

a) Number of coil turns

As the diameter of the copper wire is 0.5mm, the number of turn multiplied by 0.5mm should be less than the length of the solenoid. So the maximum number of coil turn can be defined:

$$0 \le d_c \cdot N \le l_s,\ 0 \le N \le 2l_s$$

c) Length of the solenoid

This should be longer than maximum travel range and I set upper bound as 400mm

$$R_t \le l_s \le 400mm$$

d) Length of the plunge

This should be longer than solenoid length to receive maximum electromagnetic force during the operation. So the total length of the plunge should be the sum of maximum travel range and length of the solenoid.

$$l_p = R_t + l_s$$

e) Length of the actuator

This constraint came from the total length of the linear actuator and it can be defined as:

$$l = a + l_s + R_t + t_s = a + l_s + R_t + 2$$

I set lower and upper bound for l as $0 \le l \le 500mm$, so

$$0 \le a + l_s + R_t + t_s = a + l_s + R_t + 2 \le 500$$

Also, a should be positive, so $0 \le a$

f) Travel distance

$$0 \le x \le R_t$$

g) Spring constant K

Spring generates return force and it should be larger than friction force to ensure the return of steel plunge:

$$\mu_{ss} Mg \le Kx_0$$

Steel plunger mass M can be calculated as: $M = density \times volume = 0.00805 \cdot \pi \cdot \left(\frac{d_p}{2} \right)^2 \cdot l_p$

(density of a steel = 0.00805 g/mm^3)

Finally, $0.09913 \cdot l_p \le K,\ 0.09913 \cdot (\mathrm{l}_s + R_t) \le K$

Most of the constraints came from the geometry of the linear actuator and there are two constraints related to inductance and spring constant.

3.1.4 Design variables and parameters

Objective Function

The objective function is to maximize force within the given maximum size of the linear actuator. A mathematical model has been formulated and it is as follows:

$$F = \frac{i^2}{2} \cdot \frac{a^2 \mu_0 \pi d N^2}{g_a (a+x)^2} - K(x - x_0) - \mu_{ss} Mg$$

From the aspect of x, minimum of $\mathrm{F_I}$ is generated when x is maximum. So when $x = \mathrm{R}_t$,

$$F = F_I - K \cdot \mathrm{R}_t - \mu_{ss} Mg = \frac{i^2}{2} \cdot \frac{a^2 \mu_0 \pi d N^2}{g_a (a + R_t)^2} - K \cdot \mathrm{R}_t - \mu_{ss} Mg$$

a) Design variables

#	Symbol	Description	Unit
1	a	Length between solenoid and actuator end	(mm)
2	N	Number of coil turn	
3	K	Spring constant	
4	M	Mass of the plunger	(g)
5	l_p	Plunger length	(mm)
6	l	Length of the linear actuator	(mm)
7	R_t	Maximum range of travel	(mm)

8	l_s	Length of the solenoid		(mm)

b) Design parameters

#	Symbol	Description	Value	Unit
1	d_c	Copper wire diameter	0.5	(mm)
2	g_a	Air gap	1	(mm)
3	i	Current to the inductor	3	(A)
4	d	Internal gap between shell	$d_p + 2g = 12$	(mm)
5	μ_0	Magnetic constant	$4\pi \times 10^{-7}$	(N/A^2)
6	d_p	Plunger diameter	10	(mm)
7	t_s	Outer shell thickness	2	(mm)
8	μ_{ss}	Friction coefficient between lubricated steels	0.16	
9	g	Gravitational coefficient	9.8	(Nm)
10	x_0	Initial compressed length of the spring	10	(mm)

3.1.5 Summary model

Minimize:

$$-F = -\frac{i^2}{2}\cdot\frac{a^2\mu_0\pi dN^2}{g_a(a+R_t)^2} + K(R_t - 10) + \mu_{ss}Mg = -\frac{a^2\cdot 2.1318\cdot 10^{-4}\cdot N^2}{(a+200)^2} + 190K + 0.9913(200+l_s)$$

*R_t is a linking variable, so here I set R_t with a reasonable value, 200mm

Subject to:

#	Constraints
g1	$l_s - 400 \le 0$
g2	$200 - l_s \le 0$
g3	$-N \le 0$

g4	$N - 2l_s \le 0$
g5	$0.09913 \cdot l_s + 19.826 - K \le 0$
g6	$a + l_s - 298 \le 0$
g7	$-a - l_s - 202 \le 0$
g8	$-a \le 0$

3.1.6 Initial results from an optimization

'*fmincon*' function of the MATLAB is used with SQP algorithm option for subsystem analysis. With initial condition $a = 10,\ N = 200,\ K = 5,\ l_s = 400$, function value was 68.3.

'*fmincon*' gives $a = 0.17,\ N = 200,\ K = 39.652,\ l_s = 200$ as optimal values. Also those *a, N, K,* and l_s were varied, however the optimal values presented above are global optima so results were always same with $a = 0.17,\ N = 200,\ K = 39.652,\ l_s = 200$. Then optimal function value was 188.8.

3.1.6 Sensitivity Analysis

Only g_2 and g_5 were the active constraints. g_2 is the constraint which related to l_s and K and l_s are engaged to g_5. However, since l_s (solenoid length) is directly related to the inductance of the coil, we can conclude that this subsystem is affected by inductance and spring constant. Among g_2 and g_5, g_5 has higher Lagrange multiplier value μ. It means g_5 has more impact to the subsystem compare to g_2.

Summary of sensitivity analysis

Active Constraint Functions	$\boldsymbol{\mu}$	**Relaxed Constraint**	**Diff. Optimal Value [%]**
$g_2(x) = 200 - l_s$	19.8260	$g_2(x) = 180 - l_s$	4.9997
$g_5(x) = 0.099134l_s + 19.826 - K$	190	$g_5(x) = 0.099134l_s + 15 - K$	11.56

3.1.7 Parametric study

Now we investigate the sensitivity of the optimum with respect to change in other parameters. The result is shown on the following figure, which was generated by varying each parameter

values by 10% of its nominal value while fixing the variable values at optimum.

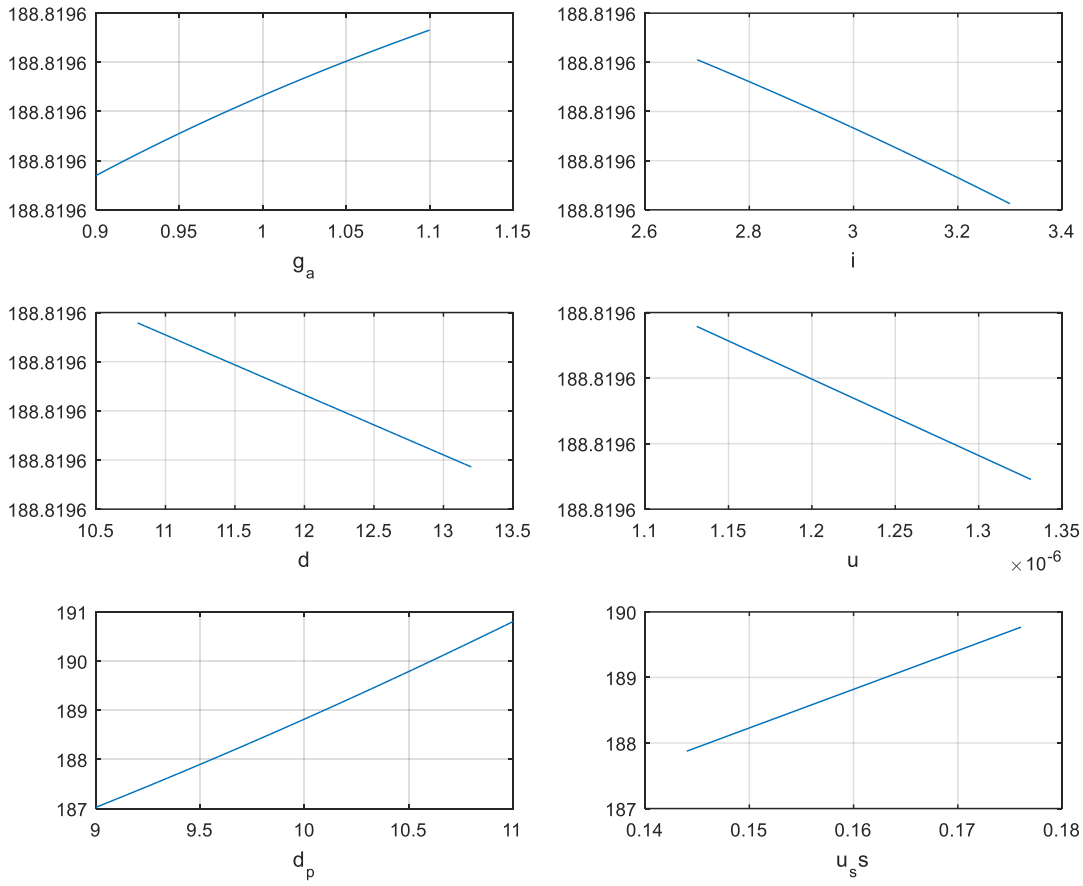

Above result indicates that the optimum is indeed affected by the changes in parameters. Especially, change in d_p and u_{ss} induces noticeable variation in the performance. The output is almost invariant to other parameters. The result immediately suggests that the system design can be improved even more if we also optimize the parameters.

3.2 Design of a Delta Robot

3.2.1 Problem Statement

Even though most of the robots in use today are serial, the parallel robots bring many benefits in mechanical motion, such as high speed, low mobile masses, high stiffness and superior accuracy. Despite its favorable characteristics, the parallel robot has some drawbacks. One of the most notable drawbacks is its relatively small workspaces. Thus, the main objective for the

sub-system is to optimize some of the geometrical features of the linear delta robot to maximize the workspace given the desired product geometry of 15 cm x 15 cm x 15 cm (total volume of 3375 cm^3) for the 3D printing.

3.2.2 Modeling

Since the three linear actuators are geometrically parallel, as shown in Figure 3.1, the cross section of the workspace perpendicular to the axis of actuator motion stays constant. Based on this finding, the linear delta robot structure was studied. An equation for finding the cross sectional workspace area was generated by considering the three circles each centered on one actuator's position have their radii equal to the lengths of the corresponding parallelogram arms. Trigonometric identities and Pythagorean identities were used to define geometric variables listed in Table 3.1 After the equation was created, the equation was transformed into its negative null form which had to be minimized in order to maximize the cross sectional area of the workspace.

Table 3.1: Nomenclature used in the linear delta robot sub-system is listed with the corresponding units.

Symbol	Description	Unit
x_1	Travel range of linear actuator 1	[cm]
x_2	Travel range of linear actuator 2	[cm]
x_3	Travel range of linear actuator 3	[cm]
L_1	Length of outer parallelogram arm (Rail 1)	[cm]
L_2	Length of inner parallelogram arm (Rail 2)	[cm]
L_3	Length of outer parallelogram arm (Rail 3)	[cm]
Y_A	Asymmetric offset of Rail 2 (y direction)	[cm]
Z_R	Separation (z direction) of Rail 1 and Rail 2	[cm]
Z_A	Asymmetric offset of Rail 1 and Rail 3 from z = 0	[cm]
Y_R	Separation (y direction) of Rail 1 and Rail 2	[cm]
A	Intersection of circle from Rail 1 and Rail 2 (y is negative)	(y, z)
B	Intersection of circle from Rail 2 and Rail 3 (y is negative)	(y, z)
A_Y	Absolute value of y coordinate value of A	[cm]

A_Z	Absolute value of z coordinate value of A	[cm]
B_Y	Absolute value of y coordinate value of B	[cm]
B_Z	Absolute value of z coordinate value of B	[cm]
α	Angle among points A, Rail 1 and Rail 3	[rad]
β	Angle among points B, Rail 2 and Rail 1	[rad]
γ	Angle among points A, Rail 2 and B	[rad]
area	Area of the workspace perpendicular to x-axis	[cm^2]

Because the range of travel, force needed to actuate and speed of linear motion is correlated with the linear actuator sub-system, it was assumed that the linear actuator allows linear motion in x-axis for the three connectors between the rails and the parallelogram arms. Then, it could be concluded that the cross section of the linear delta robot's workspace in the y-z plane is constant with some boundaries. The first boundary was created by three circles, each centered on the position of the linear actuator with a radius equal to the length of the corresponding parallelogram arms. Another boundary was the plane z = 0, through which the end effector cannot pass. Finally the cross section of the workspace could be demonstrated graphically as shown in Figure 3.2

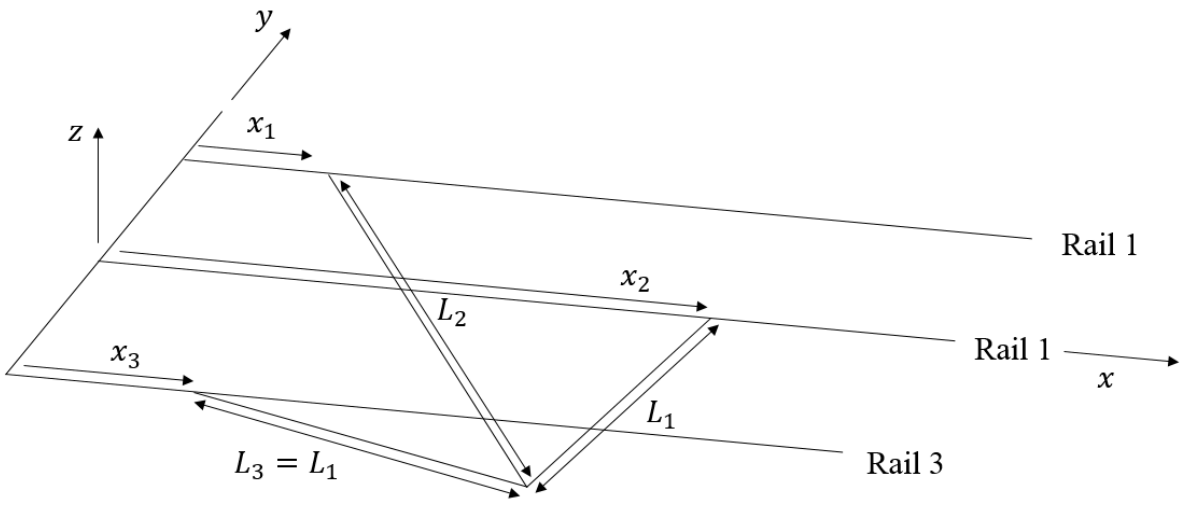

Figure 3.1: Schematic representation of the linear delta robot which contains parallel rails for the linear actuators, parallelogram arms and an extruder

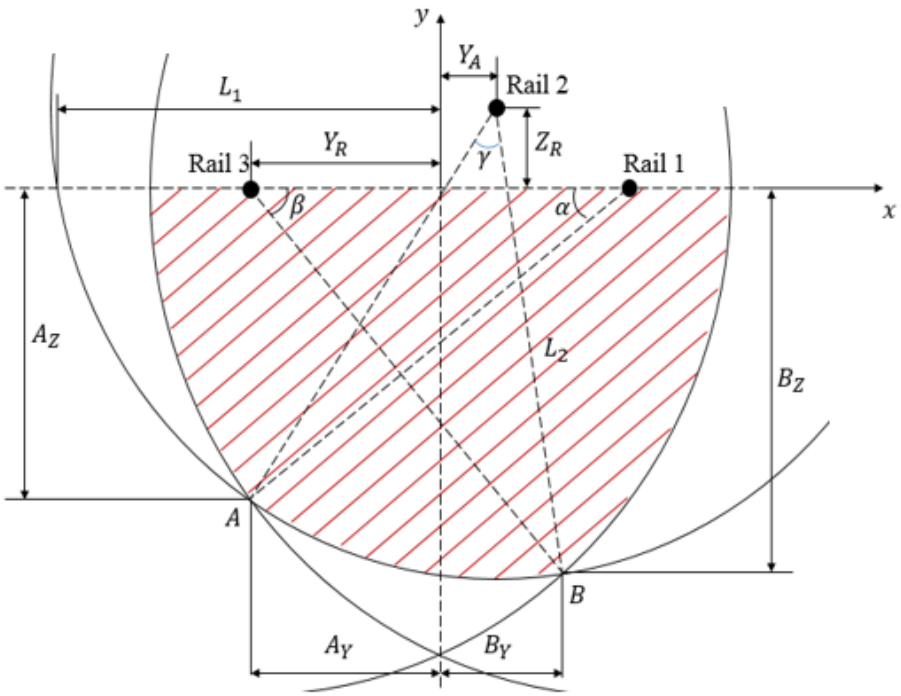

Figure 3.2: Schematic representation of the workspace cross section for the linear delta robot. The shaded region represents the cross section of the workspace.

After the set of terms and graphical representation of the workspace were generated, design variables, parameters were assigned as shown in Table 3.2 and Table 3.3. In addition, inequality constraints were created in order to assure that the optimization model was well-posed (Table 3.4). Finally, a set of equations including the equation of the workspace area was obtained (Table 3.5). The objective functions were derived mainly using the trigonometric identities and geometric identities. With the derived equations, an equation was generated to calculate the workspace cross-sectional area. The equation was transformed into its negative null form to be utilized as an objective function. Since the objective of the project is to maximize the workspace, the negative null form of the objective function was generated by taking the reciprocal of the area equation.

Table 3.2: Design variables for the sub-system model are listed.

Symbol	Description
L_1	Length of outer parallelogram arm (Rail 1)
L_2	Length of inner parallelogram arm (Rail 2)
Y_A	Asymmetric offset of Rail 2 (y direction)
Z_R	Separation (z direction) of Rail 1 and Rail 2
Y_R	Separation (y direction) of Rail 1 and Rail 2

Table 3.3: Design parameters for the sub-system model are listed

Symbol	Description	Value
Z_A	Asymmetric offset of Rail 1 and Rail3 from z = 0	0

Table 3.4: Inequality constraints for the model are presented.

Constraint Function	Constraint	Description
g1	$1 - \frac{L_1}{Y_R} \leq 0$	Outer arm length must be longer than actuator separation.
g2	$\frac{Y_A}{Y_R} - 1 \leq 0$	Actuator separation must be smaller than Asymmetric offset of Rail 2 (y direction).
g3	$-\frac{Y_A}{Y_R} \leq 0$	Actuator separation and Asymmetric offset of Rail 2 (y direction) must be positive
g4	$-\frac{L_2}{L_1} \leq 0$	Outer and central arm length must be positive
g5	$0.1 - Z_R \leq 0$	Rail 2 cannot pass through z=0 plane.
g6	$1 - \frac{L_1}{L_2} \leq 0$	Outer arm length must be larger than central arm length
g7	$4.5 - Y_R \leq 0$	Actuator separation must not be lower than 4.5 cm.
g8	$L_2 - 20 \leq 0$	Central arm length must not exceed 20 cm
g9	$L_1 - 20 \leq 0$	Outer arm length must not exceed 20 cm

Table 3.5: All equations used to derive the objective function and the objective function are summarized.

Equations	Description
$(A_Y - Y_A)^2 + (A_Z - Y_A)^2 = L_2^2$ $(A_Y - Y_R)^2 + A_Z{}^2 = L_1^2$ $(B_Y - Y_A)^2 + (B_Z - Z_R)^2 = L_2^2$ $(B_Y - Y_R)^2 + B_Z{}^2 = L_1^2$	Find $\lvert A_Y \rvert$, $\lvert A_Z \rvert$, $\lvert B_Y \rvert$, $\lvert B_Z \rvert$.
$\cos(\alpha) = \frac{Y_R + A_Y}{L_1}$ $\cos(\beta) = \frac{Y_R + B_Y}{L_1}$ $\gamma = \arcsin\left(\frac{B_Y + Y_A}{L_1}\right) + \arcsin\left(\frac{A_Y + Y_A}{L_2}\right)$	Find α, β, γ.
$\text{area} = \frac{1}{2}L_1^2(\alpha - \sin(\alpha) + \beta - \sin(\beta)) + \frac{1}{2}L_2^2(\gamma - \sin(\gamma))$ $+ (A_Y + B_Y) \times \frac{A_Z + B_Z}{2} + \frac{1}{2}A_Z(L_1 - Y_R - A_Y)$ $+ \frac{1}{2}B_Z(L_1 - Y_R - B_Y)$	Calculate workspace area.
$\min f(X) = \frac{1}{area}$	Negative null form of the objective function

3.2.3 Optimization Results

After creating a model for the sub-system, an optimization was performed using "fmincon" function of MATLAB. A set of codes used for the optimization is presented below. The optimized values of the variables and the optimal function value is also given in Table 3.6. It could be observed that the same optimal value was achieved with different initial points showing that the optimal point found is a global optimum.

Table 3.6: Summary of optimization is represented.

Variable	Initial Value	Optimized Value
L_1	12	20
L_2	12	19.58
Y_A	2	0.2711
Z_R	5	4.5
Y_R	4	0.1
area	91.74	449.8

3.2.4 Sensitivity Analysis

Based on the subsystem-level optimization results, sensitivity analysis was performed in order to further analyze the constraint functions used in the optimization. Once the optimizer returned the Lagrange multipliers for each constraint function, we could determine which constraint functions were active and inactive. Also, the magnitude of the Lagrange multipliers were compared to study the relative impact of each of the active constraint functions on the objective value. Finally, the active constraints were slightly relaxed to monitor how the objective values were affected.

Based on the optimization results, $g_5(x)$ and $g_7(x)$ were active with nonzero Lagrange multiplier values, μ. Since the Lagrange multiplier value for $g_7(x)$ was bigger, it was concluded that $g_7(x)$ would have larger impact on the optimal values. To numerically analyze the impact of each constraint, the optimizer was run with a constraint relaxed by 10 % and the change in the optimal value was monitored. As a result, the percentage difference of the optimal value for $g_5(x)$ was lower than the percentage difference for $g_7(x)$. Thus, it could be concluded that the assumption on the relative impact of each active constraint held true. The detailed summary of the sensitivity analysis is shown in Table 3.7.

Table 3.7: Summary of sensitivity analysis is presented.

Active Constraint Functions	Lagrange Multiplier, μ	Relaxed Constraint	Percentage Difference of Optimal Value [%]
$g_5(x) = 0.1 - Z_R$	$1.882e-07$	$g_5(x) = 0.09 - Z_R$	$2.171\mathrm{e}-06$
$g_7(x) = 4.5 - Y_R$	$1.929e-04$	$g_7(x) = 4.05 - Y_R$	3.909

3.2.5 Parametric Study

In addition to the sensitivity analysis on subsystem constraints, parametric study was conducted to investigate the effect of parameters on the optimal value. To numerically analyze the impact of each parameter, the optimizer was run with one parameter both increased and decreased up to 50 % and the change in the optimal value was recorded. The trend of change in the optimal value is shown in Figure 3.3. The detailed summary of the parametric analysis is shown in Table 3.8.

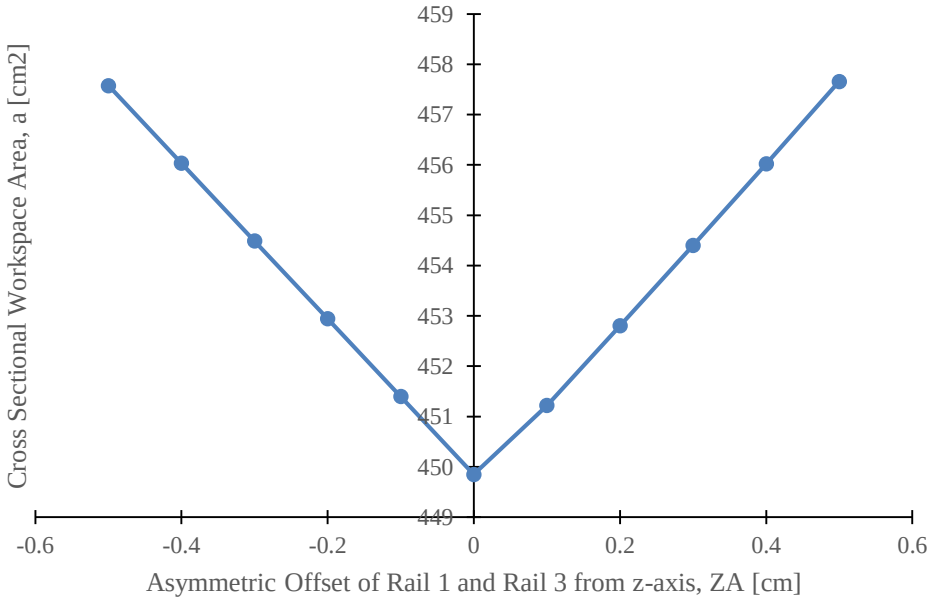

Figure 3.3: Changes in the optimal value caused by varying parameter values were plotted. It was observed that the optimal values tended to increase with a slope of 15.73 as the asymmetric offset of Rail 1 and Rail 3 from z-axis either increases of decreases.

Table 3.8: Summary of the parametric analysis which shows the percentage difference of the optimal value as the parameter was varied by ± 0.1

Parameter	Varied Parameter Value	Percentage Difference of Optimal Value [%]
$0.1 + Z_A$	0.1	4.801
$0.1 - Z_A$	-0.1	-2.285

4. SYSTEM-LEVEL OPTIMIZATION

Since the subsystem-level modeling and optimization were finished, optimization of the overall system was performed based on the results presented in previous sections. Using MATLAB's *fmincon* as the optimizer for the Multidisciplinary Feasible (MDF) approach, the global optimum was achieved using previously obtained subsystem optima as candidate initial points.

4.1 System-level Objective

System-level objective for this project was to design a linear delta robot based 3D printer which can build a 15 cm x 15 cm x 15 cm cube with minimal time. Assuming that geometric parameters were provided to limit the size of the components of the 3D printer, the main objective was to find an optimum which minimized time taken for the printer to build the cube.

To effectively 3D print the cube, we selected the route of motion for the extruder to follow as demonstrated in Figure 4.1. Assuming that the extruder resolution was 0.1 cm, the number of times the extruder had to travel back and forth was calculated using $N_{oscillation} = 15\ cm/0.1\ cm$ which led to 150 times. The result was considered to be the same for the number of layers that needed to be printed to create a 15 cm tall cube ($N_{layer} = 15\ cm/0.1\ cm = 150\ layers$). Multiplying this number by 15 cm, the width of the cube, it was found that the total distance, $\mathrm{D_{total}}$, required for the extruder to complete one layer was $2250\ \mathrm{cm}$ using $\mathrm{D_{total}} = 150 \times 15\ \mathrm{cm}$. Based on the calculated total length of travel, time required to build the entire cube was calculated using other variables including operation velocity, $\mathrm{v_{op}}$, Force generated by the linear actuator, F and moment due to the weight of the extruder, $\mathrm{M_{extruder}}$. The detailed derivation is presented in Table 4.1.

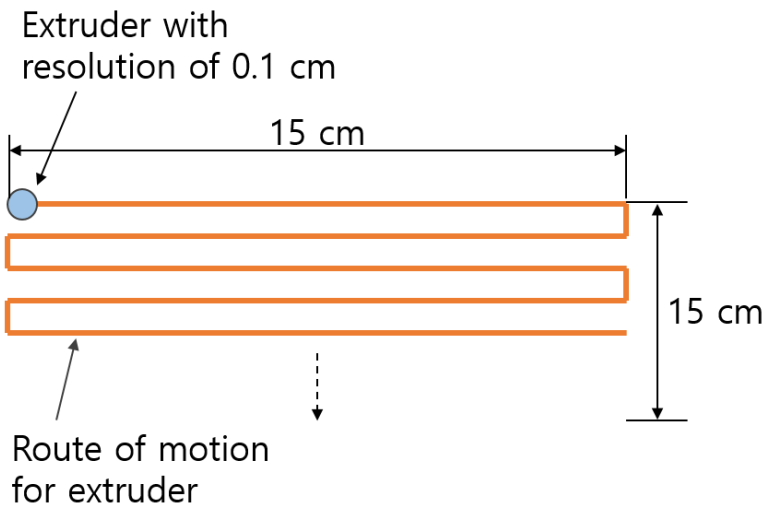

Figure 4.1: Schematic representation of the route of the extruder to build a 15 cm x 15 cm x 15 cm cube.

Table 4.1: Design variables and parameters for the system model and their types in system-level are listed.

Equations	Description
$t_a = \frac{\mathrm{m_{extruder}} v}{\mathrm{F}}$	Find time required to accelerate and decelerate the extruder from 0 to $\mathrm{v_{op}} = 5\ \mathrm{cm/sec}$. Given that the extruder's initial velocity is 0.
$\mathrm{d_a} = \frac{F t_a^2}{2 m_{extruder}}$	Find distance covered to accelerate and decelerate the extruder from 0 to $\mathrm{v_{op}} = 5\ \mathrm{cm/sec}$ assuming linear acceleration of the extruder.
$\mathrm{t_{op}} = 22500[\frac{2 m_{extruder} v}{F} + \left(15 - \frac{F t_a^2}{m_{extruder}}\right)]$	Find time of operation for the 3D printer to build a 15 cm x 15 cm x 15 cm cube.

As the first step of the modeling process, design variables were re-defined and categorized into two types; local and coupling. Also, some additional parameters such as mass of extruder, $m_{extruder}$, were defined. The variables and parameters are shown in Table 4.2. As the next step,

constraints of the system-level problem were defined. As demonstrated in Table 4.3, Equality and inequality constraints were derived from the constraints previously defined in the two subsystems. Finally, objective function was generated. Energy loss, $\mathrm{E_{loss}}$, due to acceleration and deceleration of the extruder was considered to be a countering factor against operation time required for the 3D printer to build the cube, $\mathrm{t_{op}}$, which we tried to minimize. Assigning a weighting factor, w, to each term, a cost function, f_{cost}, was created and is shown in Table 4.4.

Table 4.2: Design variables and parameters for the system model and their types in system-level are listed.

Symbol	Description	Type
L_1	Length of outer parallelogram arm (Rail 1)	Local design variable (Subsystem 2)
L_2	Length of inner parallelogram arm (Rail 2)	Local design variable (Subsystem 2)
Y_A	Asymmetric offset of Rail 2 (y direction)	Local design variable (Subsystem 2)
Z_R	Separation (z direction) of Rail 1 and Rail 2	Local design variable (Subsystem 2)
Y_R	Separation (y direction) of Rail 1 and Rail 2	Local design variable (Subsystem 2)
$\mathrm{p(x,y,z)}$	Location of extruder in x, y, z-axis	Local design variable (Subsystem 2)
$\mathrm{t_{op}}$	Operation time required to build the cube	Local design variable (Subsystem 2)
$\mathrm{M_{extruder}}$	Momentum caused by the weight of the extruder	Coupling variable ($\mathrm{y_{12}}$)
$\mathrm{R_t}$	The largest value among the three travel range values of the linear actuators, $x_1, x_2\ and\ x_3$	Coupling variable ($\mathrm{y_{12}}$)
a	Length between solenoid and actuator end	Local design variable (Subsystem 1)
N	Number of coil turn	Local design variable (Subsystem 1)
K	Spring constant	Local design variable (Subsystem 1)
M	Mass of the plunger	Local design variable (Subsystem 1)
l_p	Plunger length	Local design variable (Subsystem 1)
l	Length of the linear actuator	Local design variable (Subsystem 1)
R_t	Maximum range of travel	Local design variable (Subsystem 1)
l_s	Length of the solenoid	Local design variable (Subsystem 1)

d_c	Copper wire diameter	Local parameter (Subsystem 2)
g_a	Air gap	Local parameter (Subsystem 2)
i	Current to the inductor	Local parameter (Subsystem 2)
d	Internal gap between shell	Local parameter (Subsystem 2)
μ_0	Magnetic constant	Local parameter (Subsystem 2)
d_p	Plunger diameter	Local parameter (Subsystem 2)
t_s	Outer shell thickness	Local parameter (Subsystem 2)
μ_{ss}	Friction coefficient between lubricated steels	Local parameter (Subsystem 2)
g	Gravitational coefficient	Local parameter (Subsystem 2)
x_0	Initial compressed length of the spring	Local parameter (Subsystem 2)
$\mathrm{v_{op}}$	Operation velocity of the extruder = 5 cm/sec	System-level parameter
$\mathrm{m_{extruder}}$	Mass of extruder = 440 g	System-level parameter

Table 4.3: Equality and inequality constraints and cost function for the model are listed.

Constraint Function	Constraint
g1	$1-\frac{L_1}{Y_R}\leq 0$
g2	$\frac{Y_A}{Y_R}-1\leq 0$
g3	$-\frac{Y_A}{Y_R}\leq 0$
g4	$-\frac{L_2}{L_1}\leq 0$
g5	$0.1-Z_R\leq 0$
g6	$1-\frac{L_1}{L_2}\leq 0$
g7	$4.5-Y_R\leq 0$
g8	$L_2-20\leq 0$
g9	$L_1-20\leq 0$
g10	$l_s-400\leq 0$
g11	$200-l_s\leq 0$

g12	$-N \le 0$
g13	$N - 2l_s \le 0$
g14	$0.09913 \cdot l_s + 19.826 - K \le 0$
g15	$a + l_s - 298 \le 0$
g16	$-a - l_s - 202 \le 0$
g17	$-a \le 0$
f_{cost},	$\min f_{cost} = w_1 Time(v(x)) + w_2 E_{loss}(v(x))$ $= 0.006 \cdot 22500 \left[\frac{2m_{extruder} v}{F} + \left(15 - \frac{F t_a^2}{m_{extruder}} \right) \right]$ $+ 1$ $\cdot \frac{1}{2} \left(0.00805 \cdot \pi \cdot \left(\frac{\mathrm{d_p}}{2} \right)^2 + \mathrm{M_{extruder}} \right) (\mathrm{R_t}$ $+ \mathrm{l_s}) (\mathrm{v} - \mathrm{v_{op}})^2$

In order for the two subsystems to communicate during MDF optimization, coupling variables were required. Force generated by the linear actuator, F, was a function in terms of the largest value among the travel ranges of the linear actuators, $\mathrm{R_t}$, and force due to momentum caused by the extruder mass, $\mathrm{M_{extruder}}$ where $\mathrm{R_t}$ and $\mathrm{M_{extruder}}$ were calculated based on geometric variables from linear delta robot subsystem. Since this linear actuator force determines the acceleration and speed of the extruder, it could be concluded that operation time and energy loss were dependent upon the optimal results of the linear delta robot subsystem. The equations used to model the system-level optimization are presented in Table 4.4. As the flow chart in Figure 4.2 suggests, both of the two coupling variables are outputs of the second subsystem, linear delta robot, and inputs to the first subsystem, linear actuators.

Table 4.4: Design variables and parameters for the system model and their types in system-level are listed.

Equations	Description
$\mathrm{x_1} = x - \sqrt{L_1^2 - z^2 - (y - Y_R)^2}$ $\mathrm{x_2} = x + \sqrt{L_2^2 - (z - Z_R)^2 - (y - Y_A)^2}$ $\mathrm{x_3} = x - \sqrt{L_1^2 - z^2 - (y + Y_R)^2}$	Find the three travel range values of the linear actuators, x_1, x_2 and x_3 based on geometric variables and extruder position, $\mathrm{p(x, y, z)}$.

$\mathrm{R_t} = \max(x_1, x_2, x_3)$	Find the maximum value, $\mathrm{R_t}$, among the three travel range values of the linear actuators, x_1, x_2 *and* x_3

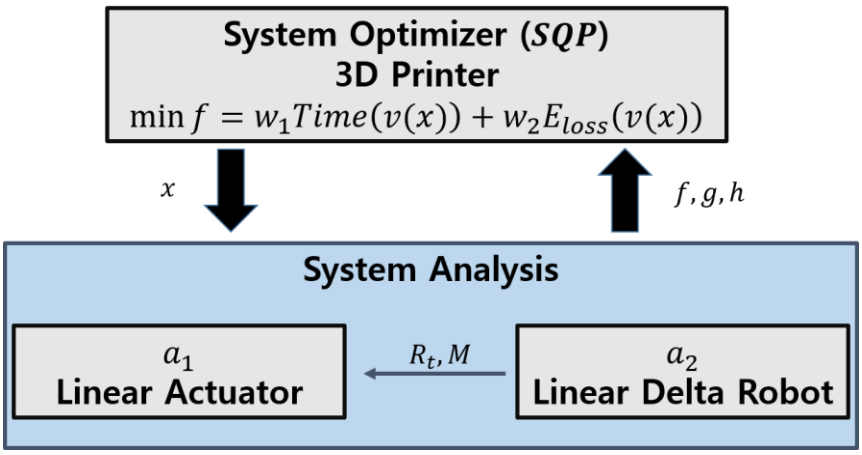

Figure 4.2: Flow chart of the project which includes the two subsystems that communicate with each other using the two coupling variables.

4.4 Optimization Results

Using the cost function and constraints defined during the modeling process, optimization was performed. As a result of the optimization, Pareto curve could be generated as shown in Figure 4.3. It could be observed that multiple optimal points could be found along the Pareto curve. We selected a possible feasible optimal point at where operation time was 4.5×10^4 and Energy loss was 1360. Using this optimal point, the optimal values of the subsystems could also be recorded as shown in Table 4.5. It could be observed that the optimal values of the Subsystem 1 had gotten worse while the optimal values of Subsystem 2 stayed the same. We believe that the optimal values of Subsystem 2 did not change, because there were no coupling variables generated by Subsystem 1 that acted as input to Subsystem 2.

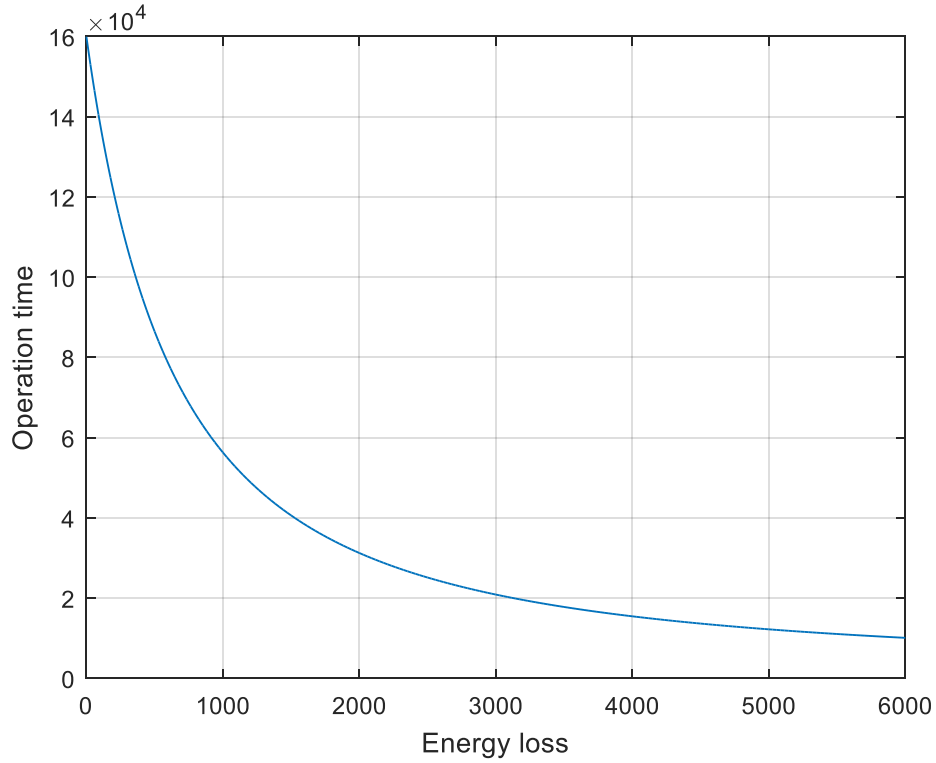

Figure 4.3: Pareto curve which shows optimal points for the two terms of the cost function, operation time and energy loss. The two terms are weighted with its corresponding weighting factors, w.

Table 4.5: Summary of optimization is listed

Variable	Initial Value	Optimized Value
L_1	20	20
L_2	19.43	19.43
Y_A	0.2328	0.2328
Z_R	4.01	4.01
Y_R	0.4	0.4
area	319.3	319.3
A	10	1.92
N	200	200
K	5	28.95
l_s	400	200
F	188.8	172.1

4.4 Sensitivity Analysis

Based on the system-level optimization results, sensitivity analysis was performed in order to further study the constraints of the system. Based on the Lagrange multipliers generated by the optimizer, we could determine which constraint functions were active and inactive. Also, the magnitude of the Lagrange multipliers were compared to study the relative impact of the active constraint functions on the objective value. Finally, the active constraints were slightly relaxed to monitor how the objective values were affected.

Based on the optimization results, $g_5(x)$, $g_7(x), g_{11}(x)$ and $g_{14}(x)$ were active with nonzero Lagrange multiplier values, μ. Since the Lagrange multiplier value for $g_{14}(x)$ was the biggest, it was anticipated that $g_{14}(x)$ would have the largest impact on the optimal value. To numerically analyze the impact of each constraint, the optimizer was run with a constraint relaxed and the change in the optimal value was monitored. As a result, the percentage difference of the optimal value for $g_{14}(x)$ was indeed the largest among the active constraints. Thus, it could be concluded that the assumption on the relative impact of each active constraint based on its Lagrange multiplier held true. The detailed summary of the sensitivity analysis is shown in Table 3.7.

Table 3.7: Summary of sensitivity analysis is presented.

Active Constraint Functions	**Lagrange Multiplier, μ**	**Relaxed Constraint**	**Percentage Difference of Optimal Value [%]**
$g_5(x) = 0.1 - Z_R$	$1.882e-07$	$g_5(x) = 0.09 - Z_R$	$4.279\text{e}-08$
$g_7(x) = 4.5 - Y_R$	$1.929e-04$	$g_7(x) = 4.05 - Y_R$	$2.940\text{e}-02$
$g_{11}(x) = 200 - l_s$	126.73	$g_{11}(x) = 180 - l_s$	2.328
$g_{14}(x) = 0.099134l_s + 19.826 - K$	394.2	$g_{14}(x) = 0.099134l_s + 15 - K$	5.384

4.5 Parametric Study

In addition to the sensitivity analysis on system-level constraints, parametric study was conducted to investigate the effect of parameters on the optimal value. To numerically analyze the impact of each parameter, the optimizer was run with one parameter both increased and decreased and the change in the optimal value was recorded. The trend of change in the

optimal value is shown in Figure 4.4. It could be observed that increasing the three parameters, $\mathrm{m}_{\mathrm{extruder}}, d_p$ and v_{op} led to an increase in operation time.

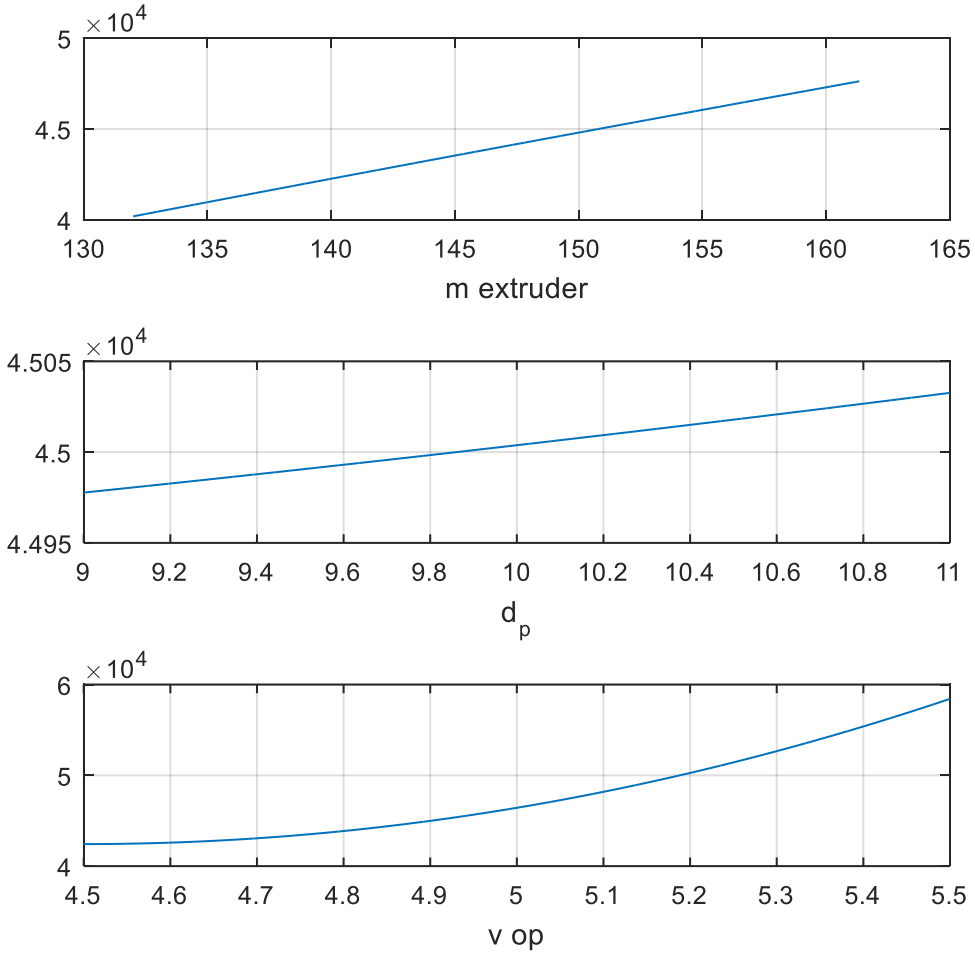

Figure 4.4: Changes in the optimal value caused by varying parameter values were plotted. It was observed that the optimal values tended to increase with a slope of 15.73 as the asymmetric offset of Rail 1 and Rail 3 from z-axis either increases of decreases.

4.6 Conclusion

By combining the two subsystems, the Pareto curve could be generated. The Pareto curve represents the possible optimal points with the two balancing factors, operation time and energy loss with their corresponding weighting factors. Picking one possible feasible optimal point, sensitivity analysis and parametric study were performed. The sensitivity analysis showed that the two active constraint functions from each subsystem were still active but with different

Lagrange multiplier values meaning that their impact on the change of the optimal value changed. The most effective constraint function was $\mathrm{g14(x)}$ with the Lagrange multiplier of 394.2. Also, the parametric study showed that the increase in the parameters also increased the optimal value, t_{op}. It would also be helpful to consider the fact that the copper coil will melt at a certain energy density factor. Adding a constraint for this factor would have led us to select a more reasonable optimal point on the Pareto curve.